Article

Life Cycle Modeling of Structural Defects via Computational Geometry and Time Series Forecasting

Sara Mohamadi [1,] * and David Lattanzi [2]

[1] Ph.D. Candidate, Dept. of Civil, Environmental, and Infrastructure Engineering, George Mason Univ., Fairfax, VA 22030; Email: smohama2@gmu.edu

[2] Assistant Professor, Dept. of Civil, Environmental, and Infrastructure Engineering, George Mason Univ., Fairfax, VA 22030 (corresponding author). ORCID: https://orcid.org/0000-0001-9247-0680; Email: dlattanz@gmu.edu

* Correspondence: dlattanz@gmu.edu

Abstract: The evaluation of geometric defects is necessary in order to maintain the integrity of structures over time. These assessments are designed to detect damages of structures and ideally help inspectors to estimate the remaining life of structures. Current methodologies for monitoring structural systems, while providing useful information about the current state of a structure, are limited in the monitoring of defects over time and in linking them to predictive simulation. This paper presents a new approach to the predictive modeling of geometric defects. A combination of segmented from point clouds are parametrized using the convex hull algorithm to extract features from detected defects, and a stochastic dynamic model is then adapted to these features to model the evolution of the hull over time. Describing a defect in terms of its parameterized hull enables consistent temporal tracking for predictive purposes, while implicitly reducing data dimensionality and complexity as well. In this study, 2D point clouds analogous to information derived from point clouds were first generated over simulated life-cycles. The evolutions of point cloud hull parameterizations were modeled as stochastic dynamical processes via autoregressive integrated moving average (ARIMA) and vectorized autoregression (VAR) and compared against ground truth. The results indicate that this convex hull approach provides consistent and accurate representations of defect evolution across a range of defect topologies and is reasonably robust to noisy measurements, however assumptions regarding the underlying dynamical process play a significant the role in predictive accuracy. The results were then validated on experimental data from fatigue testing with high accuracy. Longer term, the results of this work will support finite element model updating for predictive analysis of structural capacity.

Keywords: Remote sensing; Photogrammetry; Life cycle modeling; Time series forecasting; Structural damage; Stochastic modeling; Convex Hull; ARIMA; VAR; Fatigue crack prediction

1. Introduction

This paper presents a method for modelling the time-history evolution of defects quantified through remote sensing technologies such as laser scanning, photogrammetry, or digital imaging. The goal is to expand the use of structural assessment information commonly collected during routine inspections and improve the structural life-cycle assessment process.

Conventional structural assessments are typically based on visual inspections, embedded sensor systems, nondestructive evaluation (NDE) techniques, or some combination thereof [1–7]. In almost all cases, the goal is the nondestructive detection and identification of structural performance changes and damage, as well as to assess the reliability and safety of monitored structures[8,9]. In addition to immediate structural evaluation, these assessments ideally help engineers to estimate the remaining life of structures. This is commonly done by reviewing historical performance records and holistically

identifying temporal trends from the assessment data. However, most assessment data are not structured in a way that explicitly captures the life cycle performance of a structure, and it is therefore challenging to quantitatively evaluate the evolution of inspection data over time and carry out a predictive analysis of the future state of the structure. Life-cycle data modelling advancements could provide more precise and robust structural information, leading to better system asset management decision-making, with apparent safety and financial benefits.

1.1. Prior Work

Damage identification, localization and quantification have been extensively studied in the last decades. Using state-of-the-art NDE methods, crack can be identified and located using vibration-based methods [10–12], also large cracks and voids in concrete as well as corrosion and cracks in steel can be identified and located using ultrasonic tests[13–15]. Acoustic wave techniques can also be used to identify and locate imperfections such as the initiation of crack and the growth rate of fatigue cracks and corrosion [16], to classify crack modes in concrete[17–19] and to quantify the severity of damage [20,21]. Furthermore, it is possible to detect and locate hidden and subsurface defects using radiographic tests [22,23] and electromechanical method such as ground penetration radar [24]. Although these studies have shown the capacity to identify and assess damage to structures, the long - term contribution to structural evaluation is limited. They focus primarily on improving the accuracy of the measurement of defects and efforts have not been made to model these measured changes/defects as time-dependent phenomena.

In addition to the development of NDE and SHM techniques, there are increasing studies on the use of remote sensing and imaging technologies such as LiDAR or photogrammetry to provide new sources of inspection information. These remote sensing technologies provide high resolution 2D images or 3D point cloud models of structures, and can capture the small scale defects that are critical to understanding structural performance [25–29]. In complement to the expanding use of these technologies, there are now a variety of methods for isolating and extracting defects from 2D or 3D images[30,31], and advancements in deep machine learning methods portend future improvements [32,33]. A key advantage of these data sources is the direct link between quantified geometric changes and changes in the underlying mechanical performance that can be captured in finite element analysis, as has been evidenced by a variety of prior work [34–36]. While such capabilities provide valuable tools for structural assessment, they do not explicitly quantify life-cycle dynamics and forecasts of future defect conditions.

The question of the reliability of an engineered system has led researchers to investigate the growth of defects such as fatigue cracks and corrosion over the life-cycle of the systems. To study fatigue crack growth, model-based estimation methods such as Bayesian methods [37], Extended Kalman filtering [38] and Monte Carlo sampling [39] have been used for quantification of the estimation uncertainty. For corrosion, theoretical models and simulation tools have been developed for a better understanding of the nature of the pitting corrosion process, to allow prediction of the time evolution of maximum pit depth in corroding structures. In recent studies, stochastic approaches have also been applied to simulate corrosion [40–43]. All these efforts primarily focus on estimating the reliability of a system with given estimates of the current state of a defect, rather than quantifying the future state of defect in a way that provides a support for predictive capacity assessments.

1.2. Contribution of This Research

As stated, a critical aspect of long-term structural monitoring is the modeling of detected defects as time-dependent phenomena. Temporal modeling of defects leads to the ability to predict future defect states, and thus the future condition of the structure. While prior studies have investigated the temporal behavior of defects from an empirical perspective [44,45], efforts to quantify the dynamics of defect observations captured in remote sensing have been limited. The main objective of this study was to address these limitations for life cycle modeling of remotely sensed defects using a computational geometry approach to defect parametrization combined with time-series modeling. Presented in this paper is a novel algorithm to model the life cycle of defects manifested as either 2D

Peer-reviewed version available at Sensors 2019, 19, 4571; doi:10.3390/s19204571

or 3D point clouds. Point cloud data are a geometric representation of defects that can serve as a consistent record of the state of a structure at a given inspection interval and provide a basis for finite element analysis, among other uses [25,34]. This algorithm extracts latent features from these defect point clouds through computational geometry, fits a time-series process model to the evolution of those features, and uses stochastic forecasting model to predict future state of the defect. Consequently, a predictive analysis with regards to the future condition of the structure could be carried out by linking the modeled evolution of defects to a numerical simulation, which ultimately helps to provide a complete representation of structural performance and integrity over time. This paper does not consider the predictive analysis aspect of this process, and the readers is referred to [34–36,46] for potential applications in this domain.

The remainder of this paper is structured as follows. First, the complete analytical methodology is presented. This is followed by a presentation of synthetic experimental results designed to illustrate the key behavioral aspects of the algorithm. This is followed by experimental evaluation using fatigue crack propagation data. The paper concludes with an overall assessment of the algorithm and avenues for future work.

2. Materials and Methods

The methodology presented here consists of several steps (Figure 1). Once a defect in the structure is detected, the defect must be parametrized in a way that can support a dynamic modeling of defect evolution over time. Parameterization is achieved with feature extraction from the point cloud through computational geometric modeling of the convex hull of the cloud, resulting in a combination of hull simplexes and vertices. These parameterizations are computed for multiple time steps over the life-cycle of the structure. Once parameterized, a time-series model is fit to the sequence of parameterizations in order to capture the underlying process of evolution. This model fitting also enables the estimate the future state of the defect via out-sample forecasting. The defect shape is then reconstructed by reversing the parameterizations back to a geometric point set. While not considered in this work, this reconstructed point set can then be used to update a finite element model of the structural component based on the predicted future defect topology, leading to predictive structural assessment.

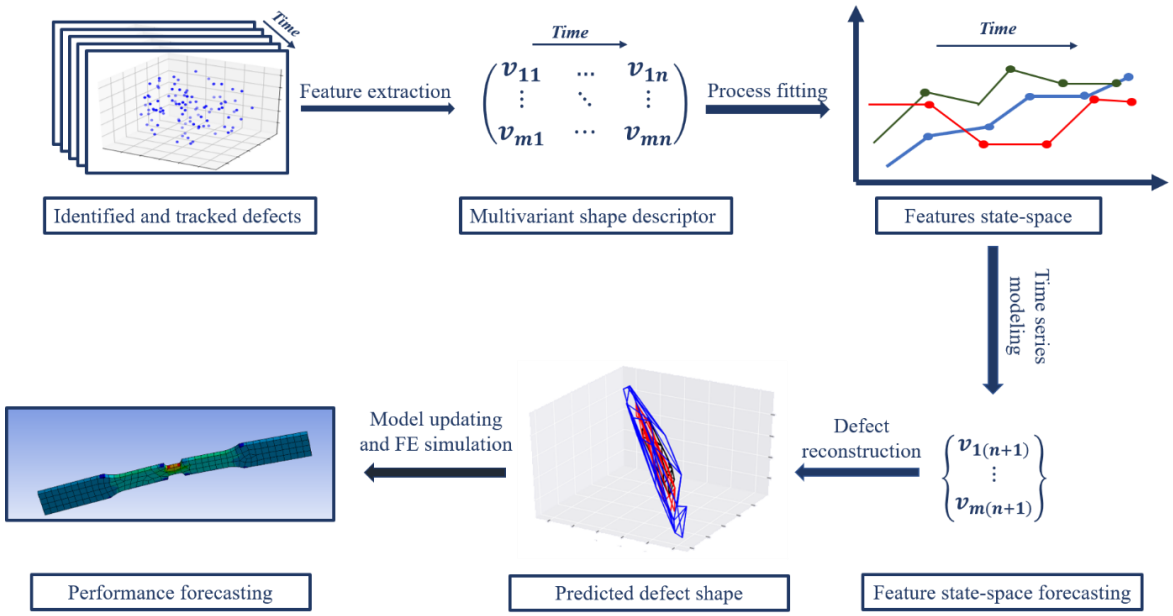

Figure 1. Schematic overview of the proposed methodology for life cycle modeling of remotely sensed defects

2.1 Defect Parameterization

Once a remotely sensed defect in a structural component has been detected through computer vision [34], the first step in the modeling process is to parameterize it so that a stochastic dynamic model can be reliably fit the extracted parameters, or "feature vector" to track the defect evolution over time. The complex nature of point cloud data necessitates this low dimensional parameterization, as tracking each individual point in a cloud would lead to an intractably high number of time-series model coefficients.

Here, we propose that the feature extraction can be done using the concept of a geometric convex hull. The convex hull of a point set is a unique representation of a point set in R^n , defined as the smallest convex polygon that surrounds all points in the point set (Figure 2) [47]. In R^3 or higher dimensional data spaces, the convex hull is similarly defined as the minimum convex polyhedron of the point set.

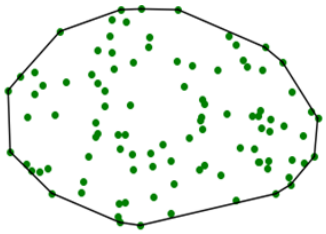

Figure 2. Convex hull of a point set in R^2

The determination of the convex hull is a geometric computation that is useful for many analyses and has been successfully applied in domains such as image processing [48] and pattern recognition [49]. Although a number of alternative feature extraction approaches were considered in this study [50,51] hull parameterization is used because of its inherent advantages. The description of a defect in terms of its parameterized hull allows for consistent temporal tracking for predictive purposes, while also reducing the dimension and complexity of the data implicitly. In addition, the convex hull concept can be extended to high-dimensional spaces to support the fusion of multiple sensors and data types, a longer-term goal of this work.

The convex hull of point cloud P is a uniquely defined convex polygon. A natural way to represent a generalized polygon is by listing its vertices in clockwise order, starting with an arbitrary starting point. As such, the problem to be solved is: given a point set $P = \{p_1, p_2, \ldots, p_m\}$ in R^n, compute a list that contains those points from P that are the vertices of the convex hull, CH(P). To find those vertices the algorithm sorts all points through a "divide and conquer" approach [52]. The convex hull algorithm finds two points with maximum and minimum spatial coordinates in a single dimension and computes a line joining these two points. This line divides the whole set into two halves. For a given half it finds the points with a maximum distance from the dividing line, forming a triangle defined by minimum and maximum point distances. Those points inside the triangle are determined to not be part of convex hull. Then, these steps are iteratively repeated to search for points with maximum distance from the separating line, until there is no point left outside of the computed triangles. The points selected at this step constitutes the convex hull. The convex hull results in a vector containing the Cartesian coordinates of the hull vertices. This extracted vector of vertices is the numerical descriptor that is later fit to a stochastic process model (Figure 3).

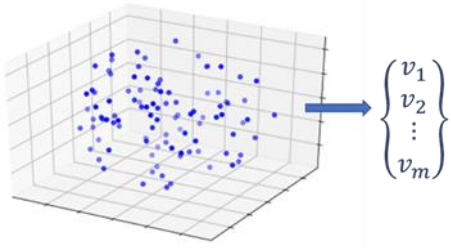

Figure 3. Feature extraction pf convex hull vertices from a 3D point cloud

2.2 Hull Time-series Modeling

Preprints (www.preprints.org) | NOT PEER-REVIEWED | Posted: 1 July 2019 doi:10.20944/preprints201907.0016.v1

Peer-reviewed version available at Sensors 2019, 19, 4571; doi:10.3390/s19204571

Once the hull vertices are extracted, the data must be presented in a time history context. Therefore, it is required that multiple stages of a defect be parameterized and compiled into a matrix of vertices representing the evolution of the defect over time. To do so, first multiple hulls computed in the previous step are aligned and registered into a common spatial reference frame. For this work, manual registration and transformation was used. However, registration can be done through approaches such as the Iterative Closest Point algorithm or by determining the 2D or 3D homography between point sets via feature-based computer vision methods [53,54]. Each vertex at $t=t_1$ is then spatially tracked. In this study, it is assumed that vertices of a hull in stage 1 ($hull_1$) are matched to their nearest neighbor (NN) vertices in $hull_2$ and likewise those are equivalent to their NN vertices in $hull_3$ and so on [55]. The nearest neighbor is found based on the smallest Euclidean distance between vertex sets. Equation 1 shows the nearest neighbor search in $Hull(Q):\{q_1, q_2, .., q_n\}$ from $p_1 \in Hull(P):\{p_1, p_2, .., p_m\}$ in 2D space ($Hull(Q)$ and $Hull(P)$ are two consecutive descriptor vectors) :

$$d(p_1, q_i) = \sqrt{(q_{ix} - p_{1x})^2 + (q_{iy} - p_{1y})^2} \quad , \tag{1}$$

At each time step, the NN of vertices in two time-steps are determined, and the change in magnitude and orientation between matched vertices is computed. Once distances and orientations between matched vertices are found, they are used for building a dataset for dynamic modeling. This dataset consists of the distances and orientations of vertex changes between subsequent hull stages throughout a time series. This dataset is illustrated for identified and aligned multiple stage of a defect with a polygon shape in Figure 4.

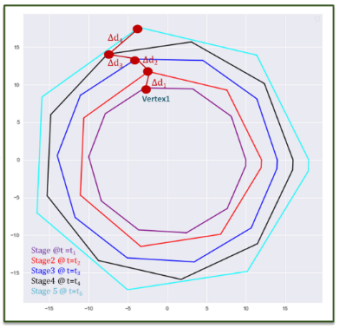

Date of Observation	$Feature_1$_Delta_Distance	$Feature_1$_Orientation	...	$Feature_m$_Delta_Distance	$Feature_m$_Orientation
Time 1	Δd_1	θ_1	...	Δd_1	θ_1
Time 2	Δd_2	θ_2	...	Δd_2	θ_2
...	...	...	...	...	...
Time n-1	Δd_{n-1}	Θ_{n-1}	...	Δd_{n-1}	Θ_{n-1}

Figure 4. Dataset representing the extracted vertices for a time-series evolution of an arbitrary polygonal defect.

2.3 Time Series Modeling

Once the dataset representing the evolution of defects has been built from previous step, a stochastic model can be fit to the dataset to model the dynamics of defect evolution. Time series forecasting is performed in order to capture the underlying long-term life-cycle trends in inspection data. The model can then be used to extrapolate the time series into the future. This modeling approach is particularly useful when the temporal behavior is stochastic, as opposed to understood deterministic evolution, and where the relationship between parameterization variables is not well understood [56]. For example, in the problem presented later in this paper, there is no knowledge available on the boundary conditions (i.e., applied load and support reactions) of the tested structural component, and there is no established deterministic model for the propagation of fatigue cracks.

There are several different approaches to time series modeling including autoregressive, moving average, exponential smoothing, ARIMA and multivariate time series VAR. All mentioned models are linear, meaning that their predictions of the future values are constrained to be linear functions of past observations. Because of their relative simplicity in understanding and implementation, linear models have been the main research focus and applied tools during the past few decades and similarly linear stochastic models were used in this study. Nonlinear modeling approaches such as recurrent neural networks were not considered here due to the limited training data available for observing defect evolution.

From the available time series models, ARIMA and VAR models were selected for this study and their performances were compared against each other. The autoregressive integrated moving average model (ARIMA) methodology developed by Box and Jenkins [57] is able to handle non-stationary time series, in other words scenarios where the statistical properties of the time series measurements do not remain constant over time. As such, it relaxes the requirement that time-series data be covariance-stationary prior to modeling, and is well-suited to the challenging variations in field conditions that impact remote sensing-based inspection practices [58]. With ARIMA, the future value of a variable is assumed to be a linear function of several past observations and random errors. ARIMA model contain two processes (autoregressive, moving average process) and explicitly includes differencing in the formulation to account for the non-stationarity of the data. ARIMA has gained enormous popularity in many areas and research practice confirms its power and flexibility [59–61]. A generalized form of the ARIMA time series model is shown in Equation 2:

$$Y_{(t)} = \phi_0 + \phi_1 \times Y_{t(-1)} + \phi_2 \times Y_{t-(+2)} + \phi_p \times Y_{t-p(+\varepsilon t)} + \theta_1 \times \varepsilon_{(t-1)} - \theta_2 \times \varepsilon_{(t-2)} - \ldots - \theta_q \times \varepsilon_{t-(q)}, \quad (2)$$

Where $Y_{(t)}$ and εt are the actual value and random error at time t, respectively. ϕ_i (i=1, 2, …, p) and θ_j (j=0,1,2, …, q) are the vectorized model coefficients. p and q are integers and often referred to as orders of the model.

As an alternative, vector autoregressive (VAR) models are effective for multivariant time series data where there is a potential dependency between model variables. Therefore, unlike an ARIMA model that estimates the present value of a variable based only on its past values, VAR models consider past values of other variables as well. This model was used here to study the dependency and effect of the movement of convex hull vertices on other verices. VAR model [62] has been used for damage detection studies previously [63,64] but it has not been any effort to model life-cycle of defect to date. The general form of autoregressive model is shown in Equation 3. Similar to ARIMA, the VAR model relates the current value of a variable to its past values.

$$Y_{(t)} = \phi_0 + \phi_1 \times Y_{(t-1)} + \phi_2 \times Y_{(t-2)} + \ldots + \varepsilon t \quad , \quad (3)$$

Where εt is random error (random shock) and ϕ_i are constants. And similarly, VAR model relates current value of a vector to its past values and each variable depends not only on its own past values but on these of other variables as well in which is K×1 random vector, ϕ_i are fixed (K×K) coefficient matrices and $\varepsilon t = (\varepsilon 1t, \ldots, \varepsilon kt)$ is K-dimensional random error [62]. To summarize, the power of ARIMA modeling stems from its ability to handle non-stationary time series with non-constant statistical properties over time. On the other hand, VAR is suitable for analyzing stationary multivariant time series with constant statistical properties and dependancy among variables .

2.3.1 Model Parameter Identification

Prior to fitting the coefficients of the time-series model, the model order must be optimized. The ARIMA model contains three components for which an order must be determined: Autoregressive (AR), Integrated (I) and Moving Average (MA) (Equation 2). The AR component uses the dependent

relationship between an observation and some number of lagged observations. The order of the AR component (p) is the number of lag observation included in the model. The Integrated component (I) employs differencing of raw observation data in order to make the time series stationary, and its order (d) is the number of times that the raw observation is differenced. The MA component uses the dependency between an observation and a residual error, and its order (q) is the size of the moving average window. In this study, ARIMA model orders (p, d *and* q) were evaluated based on a mean squared error. A prototyping dataset was divided into train and test sets and, upon the optimized combination of model orders were chosen such that they produced the least mean squared error in the test set. For the VAR model, the model order p, the number of past observations included in the model, was selected based on Hannan-Quinn information criterion (HQIC) [65]. This criterion was applied because this is used to consistently estimate the order under fairly general conditions [66] . The criterion is shown in Equation 4:

$$HQIC = -2\ln(L_{max}) + 2k\ln(\ln(n)), \quad (4)$$

where n is the number of observations, k is the number of parameters to be estimated (e.g. the Normal distribution has mu and sigma) and L_{max} is the maximized value of the log-Likelihood for the estimated model. The coefficients for k indicate the level to which the number of model parameters is being penalized. The objective is to find the model order of the selected information criterion with the lowest value HQIC value.

2.3.2 Forecasting and Defect Reconstruction

Once a model is fitted to a sequence of defect observations, the future state of the convex hull parameterizations can be predicted by the forecasting model. Once predicted, the future defect shape can then be reconstructed by converting the feature vector into a hull shape. A complication is that the number of extracted features may be inconsistent at different time steps, and this discrepancy in the length of the vectors in some cases leads to an inaccurate defect prediction. This case will happen when number of features extracted by convex hull computation at early time steps is significantly smaller than those in the later time steps. To handle this issue, a statistical assumption is employed. For features that have not been fit to a model, and therefore their values have not been predicted by dynamic modeling, the arithmetic mean of other features can be used as their expected value.

The pseudocode for the complete methodology is presented algorithm is shown in Figure 5. Upon reconstruction of the predicted geometric configuration of a defect, it is then possible to update a numerical simulation to account for the predicted change in the structure's geometry due to the defect. This updating process is not tested here, but such capabilities have been developed in prior related work, including efforts by the authors [34–36].

```
start

    #input: Point cloud of defects in time order
    #outout: The shape of defect in the next time step

    Align all point clouds and register into a common spatial reference
    For each point cloud
        Compute convex hull
        Extract vertices of hull as feature descriptors
    For each feature in feature descriptor vector at t = t0
        Search for nearest neighbor from feature vector(@t=t1) based on smallest Euclidean distance
        Store distance and angle between each pair of features
    Track those found nearest neighbors over time based on their Euclidean distance from the consequitive features vectors
    Build dataset from stored magnitude and orientation of spatial movement of features
    For each column of dataset determine model orders for timeseries model based on chosen criteria
    Build time series model with determined model order and fit the model to timeseries dataset
    Forecast variable/feature values in next time step
    Check the consistency between first and last feature vector:
        If they are consistent
            Do nothing
        Else
            Apply arithmetic mean of all predicted features as expected value of those not predicted
    Reverse the predicted features to a discrete point set and reconstruct shape of defect in next time step

end
```

Figure 5. Pseudo code for the proposed methodology

3. Experimental Validation

This section presents and discusses the results of experiments designed to evaluate the developed methodology. Two series of tests are presented. The first are a set of experiments performed on synthetic data sets. These data sets were designed to highlight key aspects of the modeling approach and provide insight into algorithm behaviors. The second set of tests are derived from laboratory scale tests of fatigue crack propagation in aluminum tensile specimens, in order to illustrate the behavior of the modeling approach in a realistic use case.

3.1 Synthetic Data Set

To initially test the accuracy and robustness of the presented methodology, synthetic 2D point clouds analogous to data derived from remote sensing (e.g. laser scanning or photogrammetry) were generated over simulated defect life-cycles. Synthetic point clouds with distribution characteristics representing different flaw topologies (e.g. rectangle, circle, and generalized polygon) were generated. Additionally, vary8ing evolution time histories were generated synthetically, representing a variety of stochastic processes (e.g. linear, quadratic, random Gaussian, and random uniform). For every combination of defect shape and stochastic process, a set of twenty defect time steps was generated. White noise was also introduced into the point clouds for each time step, in order to simulate more realistic measurements. Finally, uniform and non-uniform feature evolution were considered. Uniform feature evolution refers to a case where all vertices of the convex hull (features in the extracted descriptor vector) have the same expansion magnitude regardless of the trend of evolution. Cases where vertices were allowed to expand at varying magnitudes over a life-cycle simulation were considered non-uniform.

3.1.1 Time Series Stationarity Assessment

Time series are stationary if the statistics calculated on the time series (e.g. the mean or variance of the observations) are consistent over time. Most statistical modeling methods assume or require the time series to be stationary to be effective. There are many methods to check whether a time series is stationary or non-stationary such as reviewing a time series plot, reviewing the summary statistics for time series, or using statistical tests. The Augmented Dickey-Fuller test [67], one of the more widely used, was used in this study. It uses an autoregressive model and optimizes an information criterion across multiple different lag values. The null hypothesis (H0) of the test is that the time series can be represented by a unit root that it is not stationary (i.e. it has some time-dependent structure). The alternate hypothesis (rejecting the null hypothesis) is that the time series is stationary.

Table 1. The p-values from Augmented Dickey-Fuller test stationary test

Defect Shape / Defect Evolution	**Triangle**	**Rectangle**	**Circle**	**Polygon**
Uniform				
Linear	0.002	0.002	0.020	0.030
Quadratic	1.000	1.000	1.000	1.000
Random Uniform	0.950	0.950	0.390	0.940
Random Gauss	0.960	0.960	0.990	0.950
Non-uniform				
Random Uniform	0.950	0.950	0.96	0.990

Table 1 shows the average p-values of each generated time series, which is used in the Augmented Dickey-Fuller test to evaluate stationarity for various defect shapes and evolutions. A p-

value above 0.05 suggests that a test fails to reject the null hypothesis (H0) and it is concluded that such time series models are non-stationary. This analysis shows that all of the generated time series simulations, with the exception of the simplest linear evolution process, are non-stationary. As such, it was anticipated that the ARIMA approach would perform better than the VAR approach for the synthetic data sets.

3.1.2 Time Series Modeling

After the synthetic data sets were generated, ARIMA and VAR model orders were selected prior to fitting to time series. For the VAR models, all extracted feature vectors were input as a matrix at once and the model order (p) was set as the same for all features, whereas for the ARIMA model, each feature vector was considered individually and model order suitable to each time series were chosen based on least mean squared error. Models were then fit to the time series.

3.1.3 Metrics

The key metric for evaluating the time-series model behavior was defect reconstruction accuracy. To evaluate the results, the predicted defect shape for a future time step was compared against an established ground truth for each scenario. Two geometric metrics were computed: the percentage difference between the area of two shapes and their overlap area percentage. These two metrics were necessary in order to identify scenarios where the predicted and ground truth defect sizes were similar, but where there was a divergence in the geometric topology.

3.1.4 Results and Discussion

Table 2 and 3 show the comparison of predicted defect shapes for both the ARIMA and VAR models against the ground truth. The time series generated from linear, quadratic expansion models are defined as deterministic time series, as their future value can be exactly computed by a mathematical function. These mathematical functions are $y_t = \theta t^0$ for linear expansion, and $y_t = \theta \times d^{(t-1)}$ for quadratic expansion (θ and d are both constants). As expected, the predicted feature state from both models completely matched with the ground truth, regardless of the defect shape. The ability to forecast such a simple deterministic process is inherent to both ARIMA and VAR modeling approaches and was used to validate basic model performance.

Table 2. Comparison of predicted defect shape using ARIMA model against ground truth

Defect Shape / Defect Evolution	**Triangle**		**Rectangle**		**Circle**		**Polygon**	
Metrics	Overlap (%)	Area_Diff (%)	Overlap (%)	Area_Diff (%)	Overlap (%)	Area_Diff (%)	Overlap (%)	Area_Diff (%)
Uniform								
Linear	100	0	100	0	100	0	100	0
Quadratic	100	0	100	0	100	0	100	0
Random Uniform	100	15	100	10	100	19	89	15
Random Gauss	100	4	100	5	100	8	92	11
Non-uniform								
Random Uniform	95	7	96	5	98	4.5	87	17

More interesting results can be seen for the Gaussian and uniform random stochastic time series, which are more realistic representations of defect life-cycle dynamics in practical problems. Such stochastic processes are more challenging for any predictive model. As can be seen, ARIMA models provide relatively better prediction, though results show many similarities. The reason for the difference in predictive accuracy is the capability of ARIMA in handling nonstationary time series, as well as the assumptions of variable dependencies in VAR. Also, results show that both models can predict a defect with a Gaussian underlying process better than those with a uniform random evolution. The reason lies in the difference between the statistical properties of the two processes. Gaussian processes have a single most likely value in the distribution (the mean), whereas in uniform distributions every allowable value is equally likely, degrading predictive capabilities. Overall, the results of these synthetic experiments indicated that the convex hull parameterization approach and time series modeling provides reliable and accurate representations of defect evolution across a range of defect topologies and is reasonably robust to noisy measurements. As anticipated, ARIMA provided higher prediction accuracy as stationarity assumptions became increasingly unrealistic.

3.2 Experimental Data Set

To further evaluation of the methodology under more realistic conditions, a data set from prior experimental testing was repurposed. In these laboratory tests, aluminum tensile coupons were tested to observe fatigue crack growth under cyclic fatigue loading. Marine grade aluminum 5052-H32, with a nominal thickness of 2.29 mm was used. Specimen had machined elliptical flaw in the center and increasing load caused initiation and growth of cracks on both the right and left sides of this notch. Cycling tension loading was performed over 80k cycles and the state of crack growth was captured at 30 intermediate intervals during the test, using an inspection microscope. The captured images were then segmented to isolate the crack, and the crack patterns were transformed from pixels into point clouds (Figure 6). The convex hulls of these point clouds were computed, and features evolution were exported as time series, per the methodology delineated in Section 2. An analysis of the data sets yielded an average p-value of 0.35, indicating that the statistical uncertainty of the experimental measurements was non-stationary. Three different tests are presented in this section to evaluate the performance of the proposed methodology including single step prediction, multiple step prediction, and prediction gduring nonlinear system dynamical behavior.

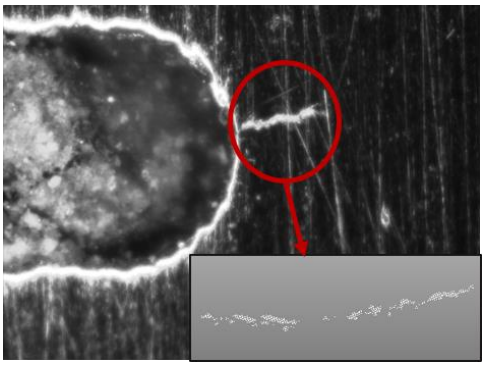

Figure 6. Extracted point cloud from the captured image

3.2.1 Single Step prediction

Performance of the proposed algorithm for predicting a single future step is evaluated in this section. Both ARIMA and VAR model were used to find the pattern of crack growth and predict the future state of crack. The convex hull of the right and left crack at 80k cycles load were computed and held out as the ground truth for one single step prediction. Results are shown in Table 4 and Figure 7. Since the performance of ARIMA and VAR model is almost the same, the predicted shape from both models has overlap and only ARIMA model can be seen in the Figure 7.

Table 4 – Comparison of predicted crack shape from ARIMA and VAR against ground truth

Preprints (www.preprints.org) | NOT PEER-REVIEWED | Posted: 1 July 2019 doi:10.20944/preprints201907.0016.v1

Peer-reviewed version available at Sensors 2019, 19, 4571; doi:10.3390/s19204571

	ARIMA		VAR	
Metric	Overlap (%)	Area_Diff (%)	Overlap (%)	Area_Diff (%)
Right Crack	100.0	7.0	100.0	7.0
Left Crack	99.0	5.0	96.0	5.0

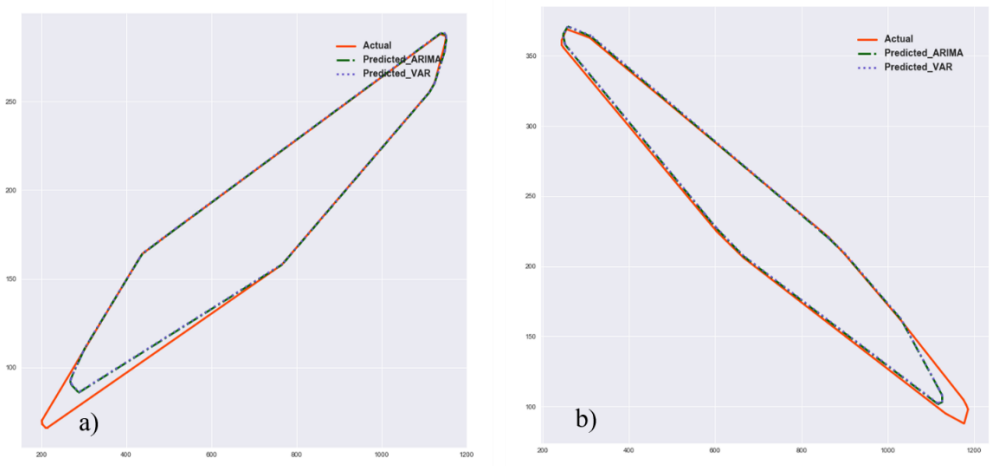

Figure 7. Comparison of the predicted crack shape against the ground truth for a) right and b) left cracks.

3.2.2 Multiple Step Prediction

To evaluate the capability of the proposed algorithm for prediction of multiple steps, 20 steps of the right-side crack, corresponding to approximately 40 thousand loading intervals, were used to fit to the ARIMA and VAR models. The true convex hulls of the crack at time steps 21 to 30 were then computed and held out as the ground truth. Then, prediction of 1 to 10 time steps were comouted and evaluated. Table 5 shows the results from the ARIMA model. Since the performance of ARIMA and VAR was very similar for this specific problem, only ARIMA is shown here.

Table 5 – Comparison of predicted crack shape from ARIMA against ground truth

	1-step	**2-steps**	**3-steps**	**4-steps**	**5-steps**
Overlap (%)	100	100	99	98	96
Area_Diff (%)	1	1	4	3	4
	6-steps	**7-steps**	**8-steps**	**9-steps**	**10-steps**
Overlap (%)	95	94	93	92	91
Area_Diff (%)	3	6	5	3	3

3.2.3 Prediction During Nonlinear System Behavior

The goal of this study was to evaluate the performance of the model during a nonlinearity in the evolution of a defect over time. For the crack fatigue problem studied here, there was a sudden change in the direction of crack growth after 48k load cycles. Of course, the predictive time series models could not accurately forecast the convex hull immediately after this event. Rather, the question here was how long it would take the time series models to correct for this nonlinearity in the dynamic evolution. The results for both ARIMA and VAR models are shown in Tables 6 and 7. As can be seen, the ARIMA model quickly adapts after only two time steps (at 50,000 load cycles). The VAR model struggles to adjust for far longer, only regaining consistent predictive accuracy after 60,000 load cycles, equivalent to an additional 4 model time steps.

Table 6. Comparison of the predicted crack shape from ARIMA model against ground truth

Load	48k	50k	52k	54k	58k
Overlap (%)	83	96	95	99	95
Area_Diff (%)	8	14	17	15	3

Table 7. Comparison of predicted crack shape from VAR model against ground truth

Load	48k	50k	52k	54k	58k	60k	62k	64k
Overlap (%)	63	70	66	92	70	95	87	97
Area_Diff (%)	8	14	17	15	16	5	2	6

3.2.2 Results and Discussion

Table 4 shows the comparison of predicted crack shape from the ARIMA and VAR models against the ground truth for cracks at the left-and right-hand side of the notch. Figure 7 shows the predicted hull shape from both models against ground truth. Results reflect that ARIMA and VAR models both provide an accurate prediction of the future state of the crack, and the presented method is able to match the convex hull of the ground truth with high accuracy. Also, the results shown in Table 5 suggest that ARIMA and VAR models are able to predict hull shape of the crack even 10 time steps ahead with reasonable, though slight degraded, accuracy However, the approach is not able to mimic the true shape of the crack. Unlike the analysis performed on synthetic point clouds in the prior section, the crack shape cannot be reasonably defined by convex polygon and therefore, convex hull parametrization cannot represent the true shape of this polygon. However, it does predict the extremis of the visible crack tip. The evaluation of the nonlinear system dynamic prediction (Table 6 & 7) shows that the ARIMA model has much better performance in adapting to nonlinear change in defect evolution and suggests that ARIMA approaches are more robust compared to VAR methods.

4. Conclusion and Future Work

In this work, a methodology to parametrize and model the dynamics of defect evolution based on a convex hull parametrization and time-series modeling was introduced. Using convex hull parametrization, 2D synthetic and experimental point clouds representing various defect shapes and stochastic evolutions were parametrized and their evolution were modeled using time series forecasting models. The future state of defects was then forecasted and evaluated against ground truth. The results indicate that this convex hull approach provides consistent and accurate representations of defect evolution across a range of defect topologies and is reasonably robust to noisy measurements, however the behavior of the underlying dynamical process plays a significant role in predictive accuracy. Predictive accuracy degrades for both ARIMA and VAR models as defect evolution becomes increasingly random, though ARIMA is slightly more robust under such conditions.

The proposed methodology has a number of advantages over current practices. First, it provides engineers with an intuitive and consistent representation of remotely sensed information over a structures' life-cycle through the reduced dimension convex hull representation. Tracking the evolution of damages and their connections to structural performance also results in more reliable forecasting capabilities and a more complete understanding of structural performance, particularly compared to existing NDE techniques that often do not quantify damage evolution through time. This process also does not require extrapolation from other data sets for prediction, rather it builds up a time-series representation based solely on the observed evolution of a given defect.

This study was part of an on-going research program and various part of the presented methodology are being considered for further improvement. The parametrizations and hull modeling are being studied for temporal tracking of non-geometric changes such as color change in structures. The hull parametrization method is being extended to high-dimensional feature space analyses, supporting

the fusion of multiple sensors and survey information for holistic life-cycle modeling. As it was presented in the methodology description, the results of this work will be used to support finite element model updating for predictive analysis of structural capacity as well. One notable avenue for future work is to adapt the algorithm to more realistically parameterize defect shape using a combination of a convex and concave hull algorithm [68]. Such an approach would allow for more accurate depiction of complex geometric topologies similar to the fatigue cracks evaluated in this work. In addition, nonlinear time series modeling methods such as Recurrent Neural Network can be studied for more complex defect evolutions, however such machine-learning driven approaches need much larger datasets to be employed.

Author Contributions: conceptualization, S.M and D.L,; methodology, S.M..; validation, S.M..; formal analysis, S.M..; resources, D.L.; writing—original draft preparation, S.M.; writing—review and editing, S.M. and D.L.; supervision, D.L.; project administration, D.L.; funding acquisition, D.L.

Funding: This work was supported in part by a grant from the Office of Naval Research (No. N00014-18-1-2014). Any opinions, findings, and conclusions or recommendations expressed in this material are those of the authors and do not necessarily reflect the views of the Office of Naval Research.

Acknowledgments: The authors would like to thank Dr. Hugh Bruck and Paul Lara (University of Maryland) for providing access to experimental data used in this work.

Conflicts of Interest: The authors declare no conflict of interest.

References

1. Sartor Richard R.; Culmo Michael P.; DeWolf John T. Short-Term Strain Monitoring of Bridge Structures. Journal of Bridge Engineering. 1999 Aug 1;4(3):157–64.

2. Shull P. Nondestructive Evaluation: Theory, Techniques, and Applications [Internet]. CRC Press; 2002 [cited 2018 May 3]. (Dekker Mechanical Engineering). Available from: https://www.taylorfrancis.com/books/9780203911068

3. Comisu C-C; Taranu N; Boaca G; Scutaru M-C. Structural health monitoring system of bridges. Procedia Engineering. 2017;199:2054–9.

4. Klikowicz P; Salamak M; Poprawa G. Structural Health Monitoring of Urban Structures. Procedia Engineering. 2016;161:958–62.

5. Clifton JR; Carino NJ. Nondestructive Evaluation Methods for Quality Acceptance of Installed Building Materials [Internet]. National Institute of Standards and Technology; 1982. Available from: http://archive.org/details/jresv87n5p407_A1b

6. Hellier C. Handbook of nondestructive evaluation. McGraw-Hill; 2001. 604 p.

7. Chang Peter C.; Liu S. Chi. Recent Research in Nondestructive Evaluation of Civil Infrastructures. Journal of Materials in Civil Engineering. 2003 Jun 1;15(3):298–304.

8. Catbas FN; Gokce HB; Gul M. Nonparametric analysis of structural health monitoring data for identification and localization of changes: Concept, lab, and real-life studies. Structural Health Monitoring. 2012 Sep 1;11(5):613–26.

9. Sohn H (Hoon); Farrar CR (Charles R); Hemez FM (François M); Czarnecki JJ (Jerry J). A Review of Structural Health Review of Structural Health Monitoring Literature 1996-2001. [Internet]. Submitted to: Third World Conference on Structural Control, Como, Italy, April 7-12, 2002. 2002 [cited 2018 Nov 8]. Available from: https://digital.library.unt.edu/ark:/67531/metadc927238/

10. Fan W; Qiao P; Vibration-based Damage Identification Methods: A Review and Comparative Study. Structural Health Monitoring. 2011 Jan 1;10(1):83–111.

11. Doebling SW; Farrar CR; Prime MB; Shevitz DW. Damage identification and health monitoring of structural and mechanical systems from changes in their vibration characteristics: A literature review [Internet]. Other Information: PBD: May 1996. 1996 [cited 2018 Nov 8]. Available from: https://digital.library.unt.edu/ark:/67531/metadc663932/

12. Gudmundson P. Eigenfrequency changes of structures due to cracks, notches or other geometrical changes. Journal of the Mechanics and Physics of Solids. 1982 Oct 1;30(5):339–53.

13. Sharma Shruti; Mukherjee Abhijit. Monitoring Corrosion in Oxide and Chloride Environments Using Ultrasonic Guided Waves. Journal of Materials in Civil Engineering. 2011 Feb 1;23(2):207–11.

14. Aranguren G; Monje PM; Cokonaj V; Barrera E; Ruiz M. Ultrasonic wave-based structural health monitoring embedded instrument. Review of Scientific Instruments. 2013 Dec 1;84(12):125106.

15. Rens Kevin L.; Greimann Lowell F. Ultrasonic Approach for Nondestructive Testing of Civil Infrastructure. Journal of Performance of Constructed Facilities. 1997 Aug 1;11(3):97–104.

16. Sagar RV; Prasad BKR. A review of recent developments in parametric based acoustic emission techniques applied to concrete structures. Nondestructive Testing and Evaluation. 2012 Mar 1;27(1):47–68.

17. Aggelis DG. Classification of cracking mode in concrete by acoustic emission parameters. Mechanics Research Communications. 2011 Apr 1;38(3):153–7.

18. Ohno K; Ohtsu M. Crack classification in concrete based on acoustic emission. Construction and Building Materials. 2010 Dec 1;24(12):2339–46.

19. Ohtsu M; Uchida M; Okamoto T; Yuyama S. Damage Assessment of Reinforced Concrete Beams Qualified by Acoustic Emission. SJ. 2002 Jul 1;99(4):411–7.

20. Zaki A; Chai HK; Aggelis DG; Alver N. Non-Destructive Evaluation for Corrosion Monitoring in Concrete: A Review and Capability of Acoustic Emission Technique. Sensors. 2015 Aug 5;15(8):19069–101.

21. Behnia A; Chai HK; Shiotani T. Advanced structural health monitoring of concrete structures with the aid of acoustic emission. Construction and Building Materials. 2014 Aug 29;65:282–302.

22. Nassr Amr A.; El-Dakhakhni Wael W. Damage Detection of FRP-Strengthened Concrete Structures Using Capacitance Measurements. Journal of Composites for Construction. 2009 Dec 1;13(6):486–97.

23. McCann DM; Forde MC. Review of NDT methods in the assessment of concrete and masonry structures. NDT & E International. 2001 Mar 1;34(2):71–84.

24. Chen Dar Hao; Wimsatt Andrew. Inspection and Condition Assessment Using Ground Penetrating Radar. Journal of Geotechnical and Geoenvironmental Engineering. 2010 Jan 1;136(1):207–14.

25. Khaloo A; Lattanzi D. Automatic Detection of Structural Deficiencies Using 4D Hue-Assisted Analysis of Color Point Clouds. In: Pakzad S, editor. Dynamics of Civil Structures, Volume 2. Springer International Publishing; 2019. p. 197–205. (Conference Proceedings of the Society for Experimental Mechanics Series).

26. Jafari B; Khaloo A; Lattanzi D. Long-term monitoring of structures through point cloud analysis. In 2016 [cited 2016 Sep 7]. p. 98052K-98052K – 8. Available from: http://dx.doi.org/10.1117/12.2217586

27. Cabaleiro M; Riveiro B; Arias P; Caamaño JC. Algorithm for beam deformation modeling from LiDAR data. Measurement. 2015 Dec;76:20–31.

28. Colomina I; Molina P. Unmanned aerial systems for photogrammetry and remote sensing: A review. ISPRS Journal of Photogrammetry and Remote Sensing. 2014 Jun;92:79–97.

29. Cabaleiro M; Riveiro B; Arias P; Caamaño JC; Vilán JA. Automatic 3D modelling of metal frame connections from LiDAR data for structural engineering purposes. ISPRS Journal of Photogrammetry and Remote Sensing. 2014 Oct;96:47–56.

30. Fleming RW; Holtmann-Rice D; Bülthoff HH. Estimation of 3D shape from image orientations. PNAS. 2011 Dec 20;108(51):20438–43.

31. Pal NR; Pal SK. A review on image segmentation techniques. Pattern Recognition. 1993 Sep 1;26(9):1277–94.

32. Kalogerakis E; Averkiou M; Maji S; Chaudhuri S. 3D Shape Segmentation With Projective Convolutional Networks. In 2017 [cited 2019 Jun 25]. p. 3779–88. Available from: http://openaccess.thecvf.com/content_cvpr_2017/html/Kalogerakis_3D_Shape_Segmentation_CVPR_2017_paper.html

33. Su H; Maji S; Kalogerakis E; Learned-Miller E. Multi-View Convolutional Neural Networks for 3D Shape Recognition. In 2015 [cited 2019 Jun 25]. p. 945–53. Available from: https://www.cv-foundation.org/openaccess/content_iccv_2015/html/Su_Multi-View_Convolutional_Neural_ICCV_2015_paper.html

595 34. Ghahremani Kasra; Khaloo Ali; Mohamadi Sara; Lattanzi David. Damage Detection and Finite-Element
596 Model Updating of Structural Components through Point Cloud Analysis. Journal of Aerospace
597 Engineering. 2018 Sep 1;31(5):04018068.

598 35. Fathi H; Dai F; Lourakis M. Automated as-built 3D reconstruction of civil infrastructure using computer
599 vision: Achievements, opportunities, and challenges. Advanced Engineering Informatics. 2015 Apr
600 1;29(2):149–61.

601 36. Yujie Yan; Burcu Guldur; Jerome F. Hajjar. Automated Structural Modelling of Bridges from Laser
602 Scanning. Structures Congress 2017 [Internet]. [cited 2017 May 12]; Available from:
603 http://ascelibrary.org/doi/abs/10.1061/9780784480403.039

604 37. Doucet A. On sequential simulation-based methods for bayesian filtering. 1998.

605 38. Myötyri E; Pulkkinen U; Simola K. Application of stochastic filtering for lifetime prediction. Reliability
606 Engineering & System Safety. 2006 Feb;91(2):200–8.

607 39. Cadini F; Zio E; Avram D. Monte Carlo-based filtering for fatigue crack growth estimation. Probabilistic
608 Engineering Mechanics. 2009 Jul;24(3):367–73.

609 40. Valor A; Caleyo F; Alfonso L; Rivas D; Hallen JM. Stochastic modeling of pitting corrosion: A new model
610 for initiation and growth of multiple corrosion pits. Corrosion Science. 2007 Feb 1;49(2):559–79.

611 41. Hong HP. Application of the Stochastic Process to Pitting Corrosion. CORROSION. 1999 Jan 1;55(1):10–6.

612 42. Caleyo F; Velázquez JC; Valor A; Hallen JM. Markov chain modelling of pitting corrosion in underground
613 pipelines. Corrosion Science. 2009 Sep 1;51(9):2197–207.

614 43. Zhou BH; Zhai ZQ. Lifetime Distribution Model of Port Facilities with Pitting Corrosion of Stochastic
615 Processes. Applied Mechanics and Materials; Zurich. 2010 Dec;44–47:46.

616 44. Mi B; Michaels JE; Michaels TE. An ultrasonic method for dynamic monitoring of fatigue crack initiation
617 and growth. The Journal of the Acoustical Society of America. 2006 Jan 1;119(1):74–85.

618 45. Vu K; Stewart MG; Mullard J. Corrosion-Induced Cracking: Experimental Data and Predictive Models.
619 ACI Structural Journal; Farmington Hills. 2005 Oct;102(5):719–26.

620 46. Fernandez I; Bairán JM; Marí AR. 3D FEM model development from 3D optical measurement technique
621 applied to corroded steel bars. Construction and Building Materials. 2016 Oct 15;124:519–32.

622 47. Berg M de, editor. Computational geometry: algorithms and applications. 3rd ed. Berlin: Springer; 2008.
623 386 p.

624 48. Rosenfeld A. Picture Processing by Computer. ACM Comput Surv. 1969 Sep;1(3):147–176.

625 49. Akl SG; Toussaint GT. EFFICIENT CONVEX HULL ALGORITHMS FOR PATTERN RECOGNITION
626 APPLICATIONS. In 1979 [cited 2018 Aug 29]. Available from: https://nyu-

627 staging.pure.elsevier.com/en/publications/efficient-convex-hull-algorithms-for-pattern-recognition-
628 applicat

629 50. Daniels JI; Ha LK, Ochotta T; Silva CT. Robust Smooth Feature Extraction from Point Clouds. In: IEEE
630 International Conference on Shape Modeling and Applications 2007 (SMI '07). 2007. p. 123–36.

631 51. Pauly M; Keiser R; Gross M. Multi-scale Feature Extraction on Point-Sampled Surfaces. Computer
632 Graphics Forum. 2003;22(3):281–9.

633 52. Barber CB; Dobkin DP; Dobkin DP; Huhdanpaa H. The Quickhull Algorithm for Convex Hulls. ACM
634 Trans Math Softw. 1996 Dec;22(4):469–483.

635 53. Besl PJ; McKay ND. Method for registration of 3-D shapes. In: Sensor Fusion IV: Control Paradigms and
636 Data Structures [Internet]. International Society for Optics and Photonics; 1992 [cited 2019 Apr 19]. p. 586–
637 607. Available from: https://www.spiedigitallibrary.org/conference-proceedings-of-
638 spie/1611/0000/Method-for-registration-of-3-D-shapes/10.1117/12.57955.short

639 54. Zhang Z. Iterative point matching for registration of free-form curves and surfaces. Int J Comput Vision.
640 1994 Oct 1;13(2):119–52.

641 55. Kleinberg JM. Two algorithms for nearest-neighbor search in high dimensions. In: Proceedings of the
642 twenty-ninth annual ACM symposium on Theory of computing - STOC '97 [Internet]. El Paso, Texas,
643 United States: ACM Press; 1997 [cited 2019 Jun 20]. p. 599–608. Available from:
644 http://portal.acm.org/citation.cfm?doid=258533.258653

645 56. Zhang GP. Time series forecasting using a hybrid ARIMA and neural network model. Neurocomputing.
646 2003 Jan 1;50:159–75.

647 57. Box GEP; Jenkins GM. Time series analysis: forecasting and control. Holden-Day; 1976. 616 p.

648 58. Box GEP; Jenkins G. Time Series Analysis, Forecasting and Control. San Francisco, CA, USA: Holden-Day,
649 Inc.; 1990.

650 59. Pankratz A, editor. Forecasting with Univariate Box-Jenkins Models [Internet]. Hoboken, NJ, USA: John
651 Wiley & Sons, Inc.; 1983 [cited 2018 Nov 7]. (Wiley Series in Probability and Statistics). Available from:
652 http://doi.wiley.com/10.1002/9780470316566

653 60. McDowall D. Interrupted Time Series Analysis. SAGE; 1980. 100 p.

654 61. Vandaele W. Applied time series and Box-Jenkins models. Academic Press; 1983. 440 p.

655 62. Lütkepohl H. New Introduction to Multiple Time Series Analysis [Internet]. Berlin Heidelberg: Springer-
656 Verlag; 2005 [cited 2018 Sep 5]. Available from: //www.springer.com/us/book/9783540401728

657 63. Yao R, Pakzad SN. Autoregressive statistical pattern recognition algorithms for damage detection in civil
658 structures. Mechanical Systems and Signal Processing. 2012 Aug 1;31:355–68.

64. Figueiredo E; Todd MD; Farrar CR, Flynn E. Autoregressive modeling with state-space embedding vectors for damage detection under operational variability. International Journal of Engineering Science. 2010 Oct 1;48(10):822–34.

65. Hannan EJ; Quinn BG. The Determination of the Order of an Autoregression. Journal of the Royal Statistical Society Series B (Methodological). 1979;41(2):190–5.

66. Hamilton JD. Time Series Analysis. Princeton University Press; 1994. 822 p.

67. Dickey DA; Fuller WA. Likelihood Ratio Statistics for Autoregressive Time Series with a Unit Root. Econometrica. 1981;49(4):1057–72.

68. Ebert T; Belz J; Nelles O. Interpolation and extrapolation: Comparison of definitions and survey of algorithms for convex and concave hulls. In: 2014 IEEE Symposium on Computational Intelligence and Data Mining (CIDM). 2014. p. 310–4.